

Advanced White cell design for investigation of ethylene using a nondispersive infrared photometer

André Eberhardt^{1,2}, Ulrich Ulmer², Katrin Schmitt², Jürgen Wöllenstein^{1,2}

¹ Department of Microsystems Engineering - IMTEK, University of Freiburg, Georges-Köhler-Allee 102, 79110 Freiburg, Germany

² Fraunhofer Institute for Physical Measurement Techniques IPM, Heidenhofstraße 8, 79110 Freiburg, Germany
andre.eberhardt@imtek.uni-freiburg.de

Abstract

Ethylene (C₂H₄) is an important marker in the ripening process of climacteric fruit and is present down to ppb concentrations. Nondispersive infrared (NDIR) sensors are suitable for the selective detection of ethylene, provided they can reach better sensitivities. This can be achieved by increasing the optical path length, e.g. using long path cells. We present an advanced White cell design, which was optimized for implementation in NDIR sensors. The design offers an optical path of 4 m, an entrance aperture of up to 5x5 mm² and a numerical aperture of 0.126. The implementation of the cell in a photometer setup for ethylene yielded a noise equivalent concentration of 860 ppb (1 σ) C₂H₄ in nitrogen (N₂).

Key words: ethylene, climacteric fruit, spectroscopy, NDIR photometer, optical long path cell

Introduction

Today up to 50% of fresh fruit and vegetables perish before they reach the customer [1]. One way to decrease these losses is the optimization of delivery and storage processes to ensure that the ripest fruits reach the customer first, first-expired-first-out (FEFO) [2]. Ethylene is suitable for this task, because it is an indicator for the ripening phase [3]. The emissions in the early ripening phases can reach the lower ppb-range. Sensors for this application must be sensitive, selective, robust and low priced. Optical NDIR sensors cover most of these criteria. The sensitivity is the only drawback of current systems. Fonseca et al. reported a detection limit of down to 10 ppm [3].

The sensitivity of these systems can be increased basically by three ways. The first is to increase the concentration using pre-concentrator units. Sklorz et al. reported an improvement of the detection limit from 40 ppm down to 700 ppb for their preconcentrator coupled NDIR photometer using a sampling time of 16 min [5]. The second way is to decrease the spectral width of the implemented interference filter in order to fit better to the main absorption peak at 10.53 μ m. But this causes a strong reduction of the remaining radiation, which is already quite weak in this region, due to the black body emission curve. The third way is to

increase the optical path of the measurement cell according to Beer-Lambert's law. This increases the sensitivity and therefore the detection limit, but has, in comparison to preconcentrating units, only a negligible influence on the complexity of the sensor.

Current work concentrated on the implementation of optical long path cells based on the design of U. White [4, 6, 7]. These cells are well suited for small sources like lasers, because the entrance aperture gets smaller and moves closer to the edge of the field mirror with increased number of foldings. This would increase the losses for large sources like black body emitters dramatically.

Hildenbrand et al. designed a White cell with an optical path of 1.5 m and reached a detection limit of about 20 ppm, which is too high for the monitoring of the fruit ripening [7]. In order to reach the required detection limit, we present an enhanced White cell design for large divergent sources, which enables a longer optical path at a simultaneously higher optical throughput.

Design of the optical long path cell

The state of the art for divergent sources are White cells. They consist of 3 spherical mirrors with identical radius of curvature. Two of these

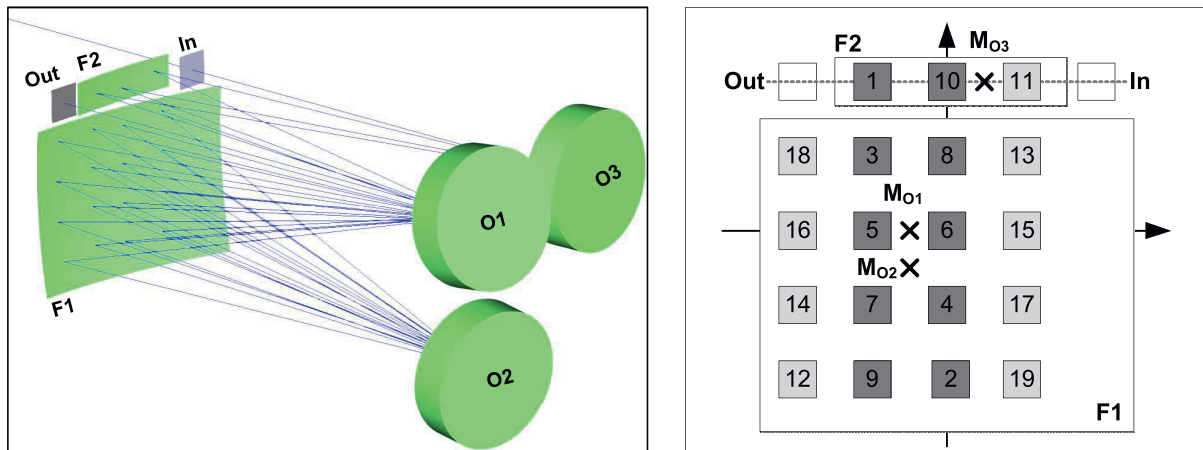


Fig. 1 (left) Optical path of the center ray in the measurement chamber. (right) Spot distribution on both field mirrors. The color indicates the iteration of the White pattern.

mirrors, the objective mirrors, are used to project images of the input aperture of the cell on the field mirror on two horizontal lines again and again. The longer the optical path gets the closer the images move together. Therefore, the permissible source diameter decreases.

The proposed design extends the classical White cell design by one field and one objective mirror (figure 1 left). It was inspired by the designs of Chernin and Glowacki et al. [8, 9]. The additional mirrors enable a matrix like spot pattern on both field mirrors F1 and F2. Objective mirrors O1 and O2 are used to create the classical 2 column pattern of White cells and objective mirror O3 in combination with field mirror F2 is used to form multiple iterations of this pattern.

The incoming radiation hits O3 first. Its center of curvature (M_{O3}) is located on F2 in the center between the desired first image (position 1 in figure 1 right) and the entrance aperture. F2 has its center of curvature in the center between O1 and O3, so the beam is guided to O1. Its center of curvature (M_{O1}) is located on F1 in order to form the second image. The distance between M_{O1} and the vertical axis of F1 determines the number of columns, which always has to be even in order to form the White patterns. The center of curvature of O2 (M_{O2}) is located directly below M_{O1} . The distance between both points is equal to the half distance between the rows on the field mirrors. The location of M_{O1} can be used to adjust the coverage of F1 and therefore the optical path by moving it up and down along the vertical axis, if the distance to M_{O2} is kept constant. The radiation is repeatedly reflected between O1, F1 and O2 in a White cell like pattern until an image falls on F2 (10). Then F2 and O3 shift the location of the Image on F2 (11) and start the next iteration of a White

pattern. This repeats until the beam hits the output of the cell.

The presented design is based on of the shelf mirrors with a radius of curvature of 100 mm. The objective mirrors have a diameter of 1". The field mirror F1 needs to have a size of at least 40x30 mm² and was cut from a 2" mirror. The second field mirror F2 has a size of 22.5x6 mm². For these configuration ray tracing simulations for 4 columns and 5 rows with an spacing of 7.5 mm in x- and y-direction and an entrance aperture of 5x5 mm² where performed using Zemax. The positions and angles were determined in the described way. But due to the short radius of curvature in comparison to the diameter of the mirrors, large deflection angles were necessary, which resulted in strong aberrations. In order to minimize these, the design was optimized numerically for smallest spot size at the output of the cell using a damped least square algorithm. The results for the center ray are presented in figure 1 left. An optical path length of 4 m and a rms-radius of 0.174 mm for a point source, located in the center of the entrance aperture, was achieved.

The body of the cell was made from aluminum and has outer dimensions of 70x70x150 mm³ with an effective cell volume of 350 ml. Both field mirrors were fixed to the front of the measurement cell. The objective mirrors were suspended with 3 degrees of freedom to adjust the position in z-direction and the angles with respect to the x- and y-axis. This enables the compensation of manufacturing tolerances like the radius of curvature of the mirrors.

Figure 2 compares the simulated (left) and achieved (right) spot pattern on both field mirrors. The photograph shows the visible part of the black body radiation of the used thermal source. The shape of the spots as well as the intensity fit very well to each other.

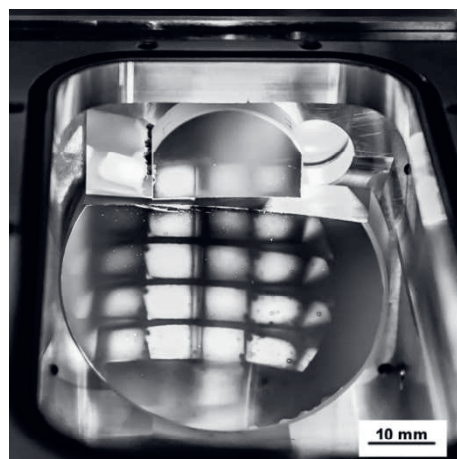
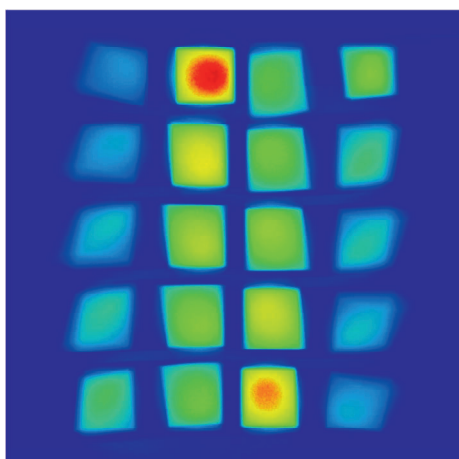


Fig. 2 Comparison of the simulated (left) and achieved (right) spot pattern on both field mirrors.

The photograph shows some artifacts, possibly caused by outshining of the entrance aperture. The aberrations could not be compensated completely. But in comparison to White cells with similar optical paths and size of the input aperture, these errors are negligible. Actually, we didn't find any solution which offered similar properties, because of the spherical aberrations introduced by the large field mirror.

Measurement setup and results

For evaluation of the performance of the designed measurement cell, it was implemented in our spectrometer setup for detection of ethylene based on a rotating interference filter [10].

This kind of spectrometer utilizes the impact of the rotation angle θ on the peak transmission wavelength λ_c of interference filters:

$$\lambda_c(\theta) = \frac{\lambda_{c,0}}{n_{eff}} \sqrt{n_{eff}^2 - \sin^2 \theta}. \quad (1)$$

It depends on the center wavelength under normal incidence $\lambda_{c,0}$, the effective refractive index n_{eff} and the rotation angle. According to equation (1) the peak transmission wavelength moves to shorter wavelengths with increasing θ . The implemented filter has a center wavelength of $10.78 \mu\text{m}$, a bandwidth of 88 nm and an effective refractive index of 2.56 . This resulted in a tuning range of about 1000 nm . Hence, the filter can be tuned over the main absorption lines at $10.53 \mu\text{m}$. A baseline fit was used to gain the absorption signal, which correlates to the gas concentration.

The optical setup of the spectrometer is shown on the left side of figure 3. The radiation of a black body source (1), Hawkeye Technologies IR-30, was modulated with a frequency of 3000 Hz using a mechanical chopper (MC2000B, Thorlabs). Two ZnSe-lenses (2)

were used to focus as much radiation as possible in to the measurement cell (3). The rotation unit (4) was placed behind the measurement cell in order to avoid beam shifting. A fast photo detector (5, PVM-2TE) was used to detect the remaining radiation. The measurement signal was forwarded to a lock-in amplifier (7265, EG&G Instruments) and the resulting magnitude signal was fed into a National Instruments measurement rack with a 24 bit DAQ card (PXI-4461). LabVIEW was used to control the measurement setup and to evaluate the measurement results.

For characterization of the system, gas cylinders with pure nitrogen (6.5) and 1000 ppm ethylene in nitrogen were used to produce concentrations between 100 ppm and 0 ppm ethylene. After each concentration a pure nitrogen step was included to monitor the baseline stability of the system. The results of an example measurement are presented in figure 3 right. A detection limit of 860 ppb (1σ) was achieved for an averaging time of 1 min . The baseline drift reached 2.9 ppb/h without compensation of any environmental effects, like temperature and pressure changes.

Discussion and outlook

An optical long path cell for use with large divergent sources, like thermal emitters, has been developed. The cell offers an optical path of 4 m for outer dimensions of $70 \times 70 \times 150 \text{ mm}^3$ and an effective cell volume of 350 ml . The cell was implemented in a rotating interference filter spectrometer for detection of ethylene in the fruit ripening process. Measurements between 100 ppm and 0 ppm revealed a detection limit of 860 ppb (1σ). In comparison to measurements with a White cell in a similar setup [10], the detection limit was reduced by a factor of 50. There are three reasons for the strong improvement. The first one is the longer

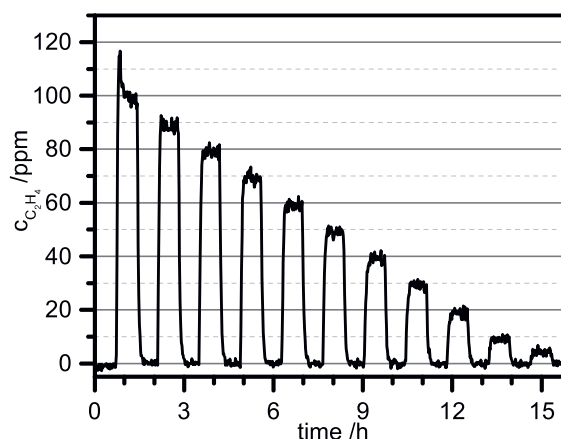
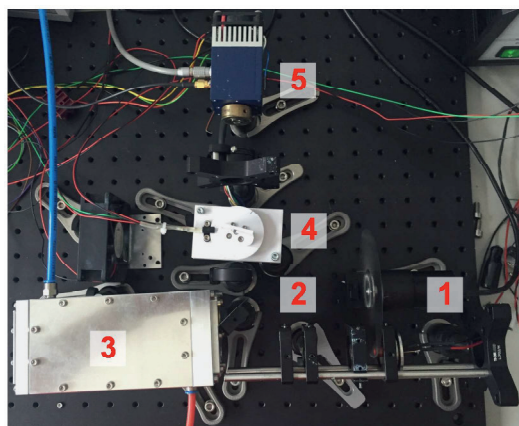


Fig. 3 (left) Photograph of the optical measurement setup: 1 - IR source and optical chopper; 2 - ZnSe lenses; 3 - measurement cell; 4 - filter rotation unit; 5 - infrared detector. (right) Example measurement of C_2H_4 in N_2 for concentrations between 100 ppm and 0 ppm.

optical path (factor 3.2) which increases the sensitivity due to Beer-Lambert's law. The second one is the much better optical efficiency of the measurement cell because of the huge entrance aperture. This overcompensated the increased reflective losses (factor 3) and the decreased numerical aperture in comparison to the White cell. Aside of the improvement of the measurement cell, the optical setup was improved to take advantage of the increased entrance aperture.

Future work concentrates on a new cell design, which is smaller and uses high efficiency gold mirrors. This increases the optical efficiency at least by a factor of 2. The optical setup will get improved with focus on smaller divergence in the filter stage in order to reduce the broadening of the bandwidth of the filter according to equation (1). In parallel, new integrated electronics with focus on low noise and speed will be developed. These improvements could easily decrease the detection limit down to the 100 ppb range.

Acknowledgements

This work was supported by a grant of the Georg H. Endress Foundation for investigation of the sustainable food production within the InnoSens project.

References

- [1] FAO, Global food losses and food waste – Extent, causes and prevention, Rome, 2011
- [2] M.L.A.T.M. Hertog, et al., Shelf life modelling for first-expired-first-out warehouse management, *Phil. Trans. R. Soc. A* 372, 20130306; doi: 10.1098/rsta.2013.0306
- [3] S. Janssen, et al., Ethylene detection in fruit supply chains, *Phil. Trans. R. Soc. A* 372, 20130311 (2014); doi: 10.1098/rsta.2013.0311
- [4] J. Fonollosa, et al., Ethylene optical spectrometer for apple ripening monitoring in controlled atmosphere store-houses, *Sens. Actuators B* 136, 546-554 (2009); doi: 10.1016/j.snb.2008.12.015
- [5] A. Sklorz et al., Merging ethylene NDIR gas sensors with preconcentrator-devices for sensitivity enhancement, *Sens. Actuators B* 170, 21-27 (2012); doi: 10.1016/j.snb.2010.11.049
- [6] J. U. White, Long Optical Paths of Large Aperture, *J. Opt. Soc. Am.* 32, 5, 285-288 (1942); doi: 10.1364/JOSA.32.000285
- [7] J. Hildenbrand et al., A compact optical multichannel system for ethylene monitoring, *Microsyst Technol* 14, 637-644 (2008); doi:10.1007/s00542-007-0475-1
- [8] D.R. Glowacki, et al., Design and performance of a throughput-matched, zero-geometric-loss, modified three objective multipass matrix system for FTIR spectrometry, *Appl. Opt.* 46 (32), 7872-7883 (2007); doi: 10.1364/AO.46.007872
- [9] S. Chernin, Promising version of the three-objective multipass matrix system, *Opt. Express* 10(2), 104-107 (2002); doi: 10.1364/OE.10.000104
- [10] A. Eberhardt, et al., Nondispersive Infrared Photometer Based on a Rotating Interference Filter for Investigation of Climacteric Fruit Ripening, *Procedia Engineering* 168, 1223-1226 (2016); doi: 10.1016/j.proeng.2016.11.423